Eur. Phys. J. C (2025) 85:646
https://doi.org/10.1140/epjc/s10052-025-14385-6

THE EUROPEAN PHYSICAL JOURNAL C

Regular Article - Theoretical Physics

Impact of quantum-corrected parameter on spinning particle motion around a black hole

Asalkhon Alimova[1,2,a], **Farruh Atamurotov**[3,b], **Ahmadjon Abdujabbarov**[4,5,c], **G. Mustafa**[6,7,d], **Phongpichit Channuie**[9,8,e]

[1] National Research University TIIAME, Kori Niyoziy 39, 100000 Tashkent, Uzbekistan
[2] Tashkent State Technical University, 100095 Tashkent, Uzbekistan
[3] Urgench State University, Kh. Alimdjan str. 14, 220100 Urgench, Uzbekistan
[4] New Uzbekistan University, Movarounnahr street 1, 100000 Tashkent, Uzbekistan
[5] School of Physics, Harbin Institute of Technology, Harbin 150001, People's Republic of China
[6] Department of Physics, Zhejiang Normal University, Jinhua 321004, People's Republic of China
[7] Research Center of Astrophysics and Cosmology, Khazar University, 41 Mehseti Street, AZ1096 Baku, Azerbaijan
[8] School of Science, Walailak University, Nakhon Si Thammarat 80160, Thailand
[9] College of Graduate Studies, Walailak University, Nakhon Si Thammarat 80160, Thailand

Received: 8 April 2025 / Accepted: 20 May 2025

Abstract The motion of spinning particles around a quantum-corrected black hole is examined in this paper. We investigate the dynamics of spinning test particles by using the Mathisson–Papapetrou–Dixon equations, the Tulczyjew spin-supplementary condition, and restricting the motion to the equatorial plane. We determine the innermost stable circular orbit (ISCO), effective potential, and effective force and examine how these depend on the black hole's α parameter and the particle's s spin. However, we also take into account a superluminal bound on the motion of the spinning particle since its kinematical four-velocity and dynamical four-momentum are not always parallel. We also show how the parameter α affects the maximum value of the spin parameter s. We determine the critical angular momentum of the particle for which a collision is possible by investigating collisions of spinning particles close to the horizon of a black hole. Finally, we compute the particle's center-of-mass energy $\mathcal{E}_{cm}$ and analyze how the spin of the colliding particles affects it.

1 Introduction

The black holes (BHs) are the most intriguing and fascinating objects in the Universe. The gravity of the BHs is dominating over all other interactions; thus, they play a role of cosmic laboratory for gravitational physics. General Relativity (GR) proposed by Einstein in 1915 properly describes the gravitational effects surrounding BH. Most of the existing experiments and observations are consistent with GR and adequately describe the effects around BH. Recent observation of the shadow of a supermassive BH [1,2] and detection of gravitational waves [3] can be considered as a test of GR in the strong-field regime. However, GR meets fundamental issues as a classical field theory. Particularly, the existence of singularity at the origin of classical solutions of GR and inconsistency with the quantum field theory require one to consider further modifications of GR or alternative theories of gravity. Fortunately, the current resolution of the experiments and observations used to test GR allows one to consider such modifications.

In the literature, there exist a large number of modified and alternative theories of gravity. In order to sort out these theories, one needs to develop corresponding tests of the particular theory. The huge number of theories creates an additional problem related to the degeneracy issues: the parameters of different theories/models may mimic each other. In order to resolve this issue, one needs to develop independent experimental/observational tests. Other ways of solving this prob-

[a] e-mail: asalxon2197@gmail.com
[b] e-mail: atamurotov@yahoo.com
[c] e-mail: ahmadjon@astrin.uz
[d] e-mail: gmustafa3828@gmail.com
[e] e-mail: phongpichit.ch@mail.wu.ac.th (corresponding author)

Published online: 11 June 2025

lem can be performed by introducing the parameterization of the space-time metric [4–6].

No hair theorem claims that the solution of field equations describing BH may carry only three parameters: mass M, angular momentum J, and electric charge Q [7,8]. Possible modifications of GR may be related to the reconsideration of this theorem and include additional charges of BH, which may lead to the quantum hair [9]. One of the possible quantum hair of BH is considered in Ref. [10] where the authors have found that trivial deformations of the seed Schwarzschild vacuum preserve the energy conditions and provide a new mechanism to evade the no-hair theorem. Thermal analysis and thermal fluctuations of this solution have been explored in Refs. [11,12]. Different astrophysical scenarios have been studied to bypass the no-hair theorem in Refs. [13–18]). Other works devoted to the analysis of hairy BH can be found in [19,20].

The motion of particles around compact gravitating objects may be used as a useful tool to test gravity theories. In metric theories of gravity, test particles follow the geodesics, and thus the trajectories of the particles may provide information about the physical parameters of the central object. On the other hand, particles with non-zero spin parameters will be deflected form geodesics due to interaction of spin and curvature of the spacetime. The exploration of the spinning particles motion may provide more information about space-time structure. The investigations of the dynamics of neutral, charged, magnetized particles around compact objects in different models can be found in Refs. [21–31]. Moreover, the electromagnetic field around the compact object may have new effects on the motion of charged / magnetized particles [32–35]. The study of the interaction of the spin of the particle with the background geometry may be found in Refs. [36–50].

The dynamics of non-zero spin particles can be explored using MPD [51]. Mathisson-Papapetrou-Dixon (MPD) equations contain terms that are responsible for the interaction of the spin tensor and the curvature tensor. One of the main features of the spin-particle dynamics is spin precession [52–54].

The particle dynamics may lead to the energetic of the BH. In particular, BHs may play the role of particles accelerator. In Ref. [55] it has been shown that for fine-tuned values of the parameters of the particles and extreme rotating BH the center of mass energy of two colliding particles may diverge. This mechanism is referred to as the BSW mechanism after the authors (Banados, Silk, and West). Here, we plan to analyze the collision of two spinning particles in the vicinity of quantum corrected BH. The effect of the modifications to gravity theory on the spin-particle dynamics has been explored in [44,56–58]. Recent studies have explored the motion of charged, spinning, and magnetized test particles around quantum improved charged black holes, highlighting the significant effects of quantum corrections on their orbital dynamics [59].

We intend to investigate the dynamics of spinning particles in the vicinity of the quantum-corrected BH characterized by the solution presented in [60]. The paper is structured as follows. We examine the solution of a quantum-corrected BH in Sect. 2.1. Section 2.2 is dedicated to the examination of the equations of motion for spinning particles in a generic context. The behavior of spinning particles around quantum-corrected BHs has been examined in Sect. 3. We regard the spinning particle collision discussed in Sect. 4 as a significant application of particle dynamics. We summarize our findings in Sect. 5. We employ a geometrical unit system in which $G = 1 = c$ and the space-time signature is $(-,+,+,+)$. Latin (Greek) indices range from 1(0) to 3.

2 Basic equation of motion

2.1 Quantum corrected black hole

The classical BH solutions are altered by quantum corrections, which may cause variations in the behavior of nearby particles. By adding higher-order terms in the curvature to the Einstein-Hilbert action, the effective field theory approach introduces one such correction. We aim to examine the dynamics of spinning particles near the quantum-corrected black hole, described in spherical coordinates by the solution presented in [60,61].

$$ds^2 = -f(r)dt^2 + f(r)^{-1}dr^2 + r^2d\theta^2 + r^2sin^2\theta d\phi^2. \quad (1)$$

In the above equation $f(r)$ representing the lapse function, which is further defined as:

$$f(r) = \left(1 - \frac{2M}{r} + \frac{\alpha M^2}{r^4}\right), \quad (2)$$

where M represents the Arnowitt–Deser–Misner mass, and $\alpha = 16\sqrt{3}\pi\gamma^3 l_P^2$ is a parameter influenced by quantum corrections. In this expression, γ denotes the Immirzi parameter which measures the size of the quantum of area in Planck units while l_P refers to the Planck length [62]. The quantum corrections introduce a minimum mass $M_{\min}$ for the quantum-corrected BH. This solution originates from the quantum extension of the Oppenheimer–Snyder model in the framework of Loop Quantum Cosmology. For simplicity, we use the dimensionless parameter $\hat{\alpha} = \alpha/M^2$ instead of α throughout this work. When $\hat{\alpha} = 0$, the Eq. (1) simplifies to the line element of a standard Schwarzschild BH. $\hat{\alpha}$ must be less than $\frac{27}{16}$ for a quantum-corrected BH to exist. It is obvious from Fig. 1 that for the values $\hat{\alpha} > \frac{27}{16}$ a horizonless configuration arises.

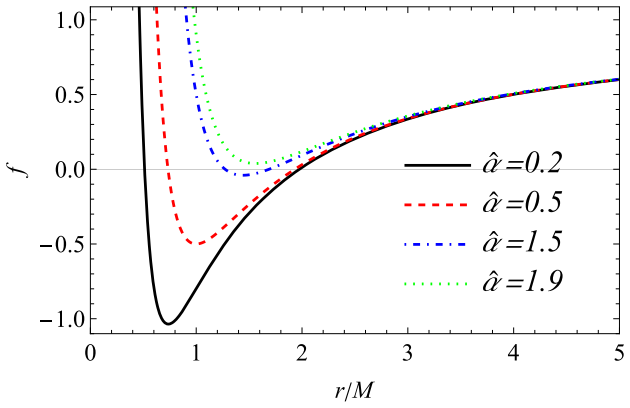

Fig. 1 The radial dependence of the lapse function for different values of the parameter $\hat{\alpha}$

2.2 Equations of motion for a spinning particle

Spinning particles move in significantly different ways compared to non-spinning ones. While spinning particles follow differential equations with additional variables related to the connection between the Riemann curvature tensor and the particle's spin, non-spinning particles follow the geodesic equation within the specified background geometry. The set of differential equations for describing the motion of massive spinning particles is called the MPD equations [52,53] and has the following form:

$$\begin{aligned} \frac{Dp^{\alpha}}{d\lambda} &= -\frac{1}{2}R^{\alpha}{}_{\beta\delta\sigma}u^{\beta}S^{\delta\sigma}, \\ \frac{DS^{\alpha\beta}}{d\lambda} &= p^{\alpha}u^{\beta} - p^{\beta}u^{\alpha}, \end{aligned} \tag{3}$$

where $D/d\lambda \equiv u^{\alpha}\nabla_{\alpha}$ is the projection of the covariant derivative along the trajectory of the particle as $u^{\mu} = dx^{\mu}/d\lambda$ is the test particle's 4-velocity, p^{α} is the canonical 4-momentum, $R^{\alpha}{}_{\beta\delta\sigma}$ is the Riemann curvature tensor, λ is an affine parameter and $S^{\alpha\beta}$ is the antisymmetric spin tensor: $S^{\alpha\beta} = -S^{\beta\alpha}$. Alternatively, when the components of

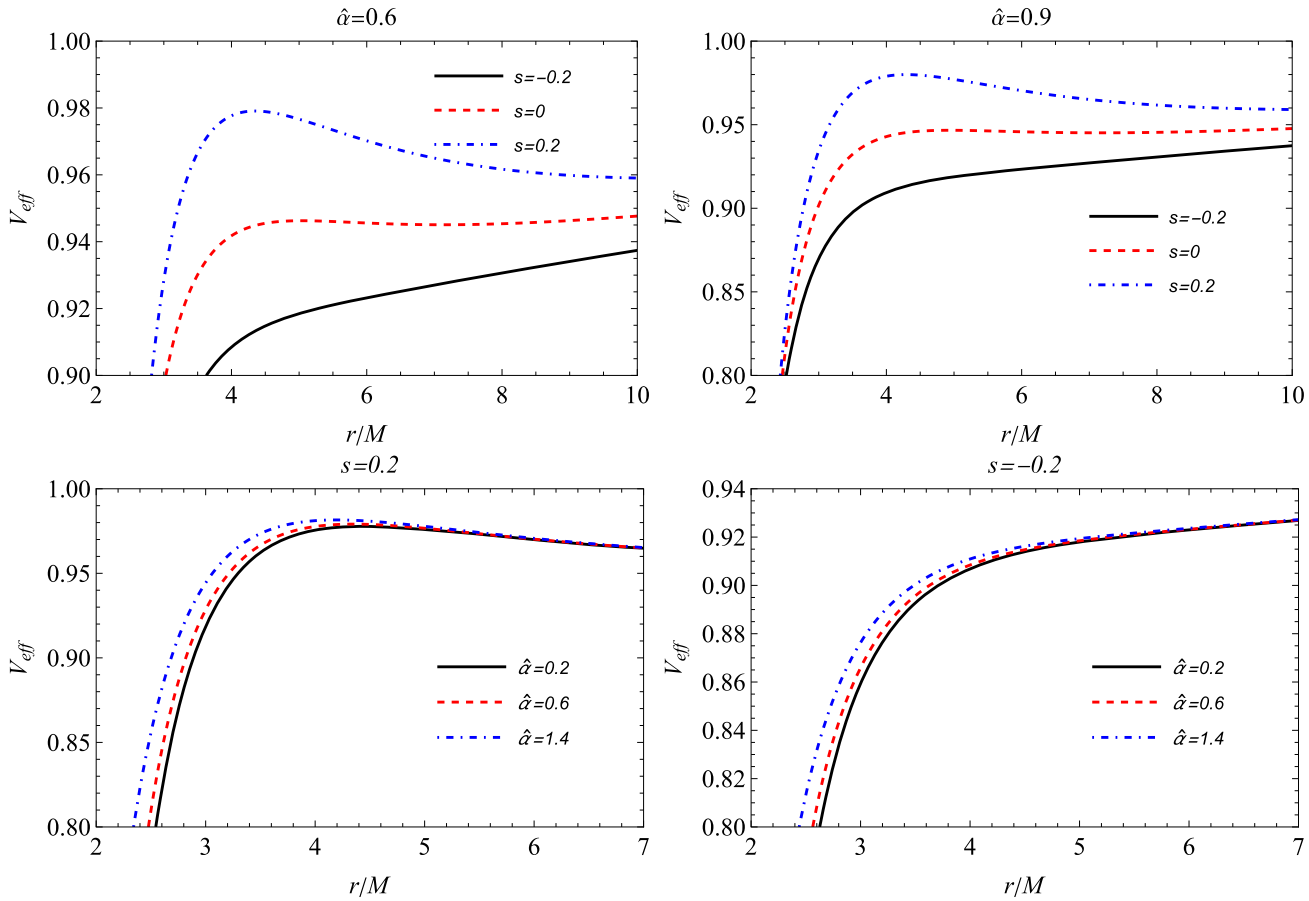

Fig. 2 The radial dependence of the effective potential, V_{eff}, for varying parameter sets. The upper row illustrates the behavior of V_{eff} for fixed values of the parameter $\hat{\alpha} = 0.6$ and 0.9, with different spin values $s = -0.2, 0, 0.2$. The lower row highlights fixed spin values $s = -0.2$ and 0.2, while varying $\hat{\alpha} = 0.2, 0.6, 1.4$

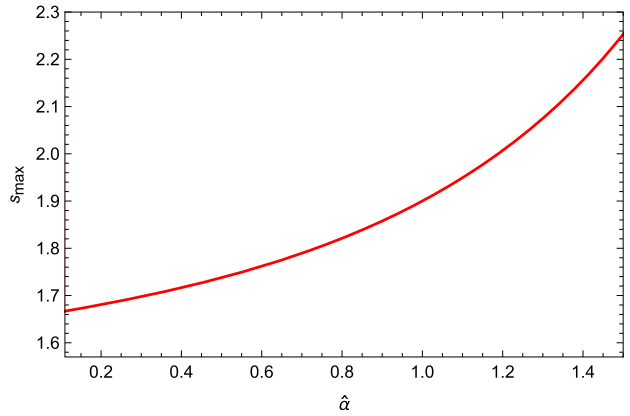

Fig. 3 Maximal value of spin parameter dependence of $\hat{\alpha}$

$S^{\mu\nu}$ are null, the differential equation simplifies as:

$$\frac{Dp^{\mu}}{d\tau} = 0. \tag{4}$$

The center of mass of the spinning test particle is an essential component of the MPD equations. In this sense, to solve the system in Eq. 3, one needs to fix its center of mass [63]. Although a particle is point-like, its motion is defined in relation to the center of mass. This is especially essential to mitigate uncertainty in predicting the dynamics of spinning particles from the following condition:

$$S^{\alpha\beta} p_{\alpha} = 0. \tag{5}$$

The Tulczyjew spin supplementary condition (SSC) is the name given to this situation.The SSC relation and the MPD equations yield two independent conserved quantities: the canonical momentum and the particle's spin, as defined by the following relations:

$$\begin{aligned} S^{\alpha\beta} S_{\alpha\beta} &= 2S^2, \\ p^{\alpha} p_{\alpha} &= -m^2. \end{aligned} \tag{6}$$

Now, by using Eq. (3), one can introduce the following quantity

$$\mu = -P^{\beta} u_{\beta}. \tag{7}$$

Further, Eq. (3) gives the relation as:

$$P^{\alpha} = \mu u^{\alpha} - u^{\beta} \frac{DS^{\alpha\beta}}{D\lambda}. \tag{8}$$

The above expression indicates that the momentum and velocity vectors are no longer parallel for spinning particles.

Moreover, along with the SSC-dependent conserved values, there exist standard background-dependent conserved quantities linked to the Killing vectors. In an axially symmetric space-time, two Killing vector fields exist. One belongs to invariant time translations ξ^{α}, while the other allows rotations about the azimuthal angle ϕ, ψ^{α}. These quantities can be calculated using the following equation:

$$p^{\alpha}\kappa_{\alpha} - \frac{1}{2} S^{\alpha\beta} \nabla_{\beta} \kappa_{\alpha} = p^{\alpha}\kappa_{\alpha} - \frac{1}{2} S^{\alpha\beta} \partial_{\beta} \kappa_{\alpha} = \text{constant}, \tag{9}$$

where k^{α} represents the two Killing vector fields: ξ^{α} and ψ^{α}.

2.3 Superluminal bound

It is worth mentioning the fact that spinning particles should have a constraint for the values of spin, a superluminal constraint, above which the velocity of the particle exceeds the speed of light, which is non-physical.This is because the four-velocity u^{α} and the four-momentum p^{α} are not parallel. The four-velocity of the particle u^{α} is not time-like, but the four-momentum p^{α} is clearly a conserved quantity (see Eq. (6)) and always time-like. As a result, the normalization requirement $u^{\alpha}u_{\alpha} = -1$ is not sufficiently satisfied and the values of the normalization condition may be positive for certain spin values s. As a result, the particle's motion loses its physical significance and takes on the appearance of space-like.

The following restriction must be applied (on the equatorial plane) in order to maintain the trajectory of spinning test particles with time-like character:

$$\frac{u_{\alpha}u^{\alpha}}{(u^t)^2} = g_{tt} + g_{rr}\dot{r}^2 + g_{\varphi\varphi}\dot{\varphi}^2 \leq 0. \tag{10}$$

In this case, the derivative with respect to the time coordinate t is indicated by the dot. The following form represents the expressions for dr/dt and $d\varphi/dt$ obtained by solving the MPD equations:

$$\begin{aligned} \frac{dr}{dt} &= \frac{u^r}{u^t} = \frac{\mathcal{C} p_r}{\mathcal{B} p_t}, \\ \frac{d\varphi}{dt} &= \frac{u^{\varphi}}{u^t} = \frac{\mathcal{A} p_{\varphi}}{\mathcal{B} p_t}, \end{aligned} \tag{11}$$

where

$$\begin{aligned} \mathcal{A} &= g^{\varphi\varphi} + \left(\frac{S^{\varphi r}}{p_t}\right)^2 R_{trrt}, \\ \mathcal{B} &= g^{tt} + \left(\frac{S^{\varphi r}}{p_t}\right)^2 R_{\varphi rr\varphi}, \\ \mathcal{C} &= g^{rr} + \left(\frac{S^{\varphi r}}{p_t}\right)^2 R_{\varphi tt\varphi}. \end{aligned} \tag{12}$$

To determine the *superluminal bound*, we establish the function $\mathcal{F} = u_{\alpha}u^{\alpha}/(u^t)^2$ and investigate three cases:

- if $\mathcal{F} < 0$, the particle's journey is time-like and the spin values are physical.
- if $\mathcal{F} = 0$, there is a superluminal bound (the critical values of spin s_{max}).
- if $\mathcal{F} > 0$, the spinning test particle follows a space-like trajectory with non-physical spin values (forbidden).

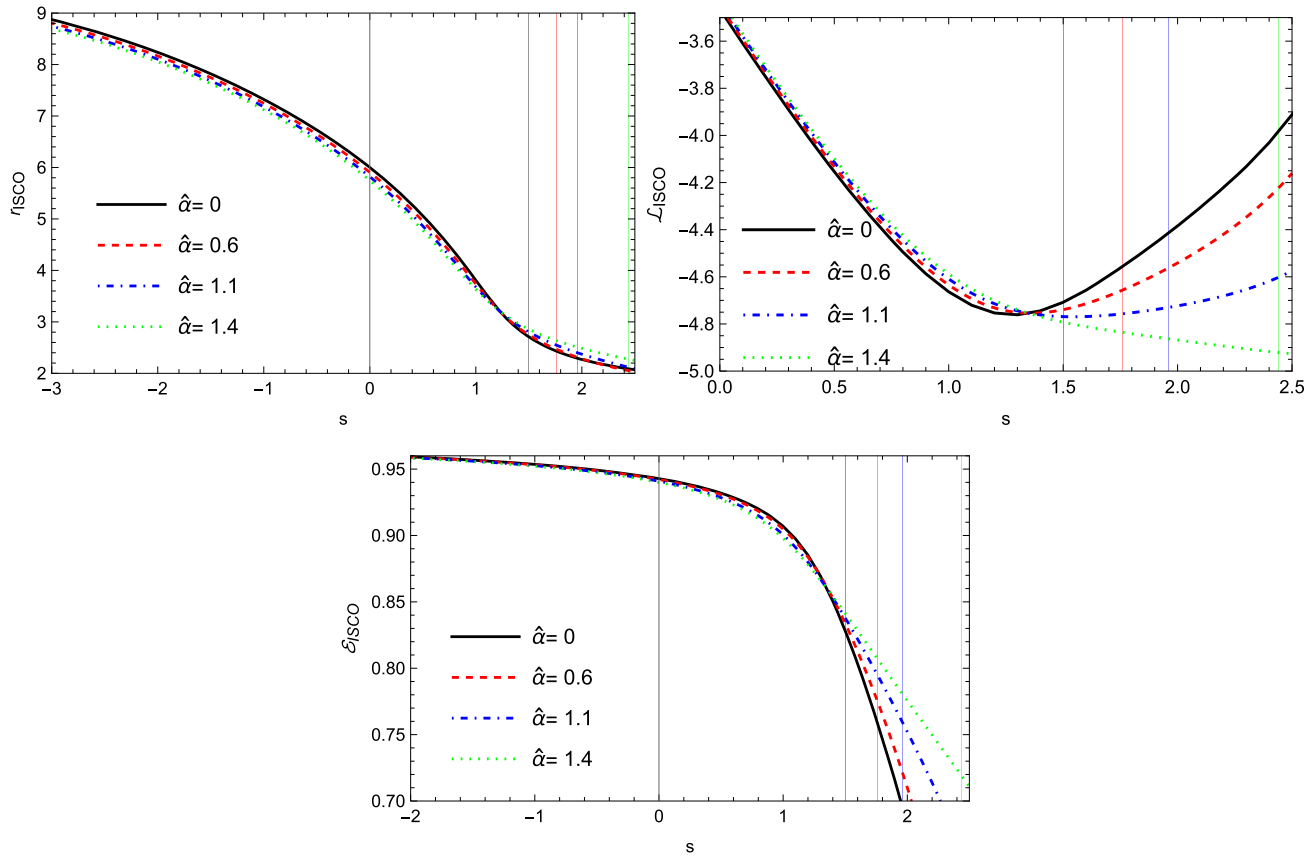

Fig. 4 The variation of the radius, specific angular momentum, and energy at ISCO for fixed values of $\hat{\alpha}$ in spin parameter s

To put it simply, the superluminal bound is the threshold that distinguishes space-like trajectories from time-like ones. The spin values of the test particle are valid until the function vanishes $\mathcal{F} = 0$. This is because, according to condition Eq. (10), positive values of $\mathcal{F}$ indicate that the test particle may have a velocity that exceeds the speed of light c, which is non-physical. The second condition mentioned above yields the critical values of the spin s_{max}.

3 Dynamics of spinning particles around quantum corrected black hole

3.1 The effective potential

In the preceding section, we examined the fundamental principles of the equations that describe the motion of a spinning particle. This section focuses on the analysis of spinning particle dynamics within the specified metric (Eq. (1)).

Initially, we aim to determine the effective potential of a rotating test particle in the vicinity of a quantum-corrected BH. In order to simplify the equation, we examine the motion within the equatorial plane ($\theta = \pi/2$).

In static and spherically symmetric spacetimes, there exist two conserved quantities: energy E and total angular momentum J (where $J = L + S$), with S representing spin and L representing orbital angular momentum. Further, these both quantities are defined as:

$$\begin{aligned} -E &= p_t - \frac{1}{2} g_{tt,r} S^{tr} \\ J &= p_\phi - \frac{1}{2} g_{\phi\phi,r} S^{\varphi r}, \end{aligned} \tag{13}$$

Furthermore, considering particle's motion is constrained to the equatorial plane, the antisymmetric spin tensor $S^{\alpha\beta}$ has just two independent components [64] which are expressed as:

$$\begin{aligned} S^{tr} &= \frac{p_\phi s}{\sqrt{-g_{tt} g_{rr} g_{\phi\phi}}}, \\ S^{\varphi r} &= -\frac{p_t s}{\sqrt{-g_{tt} g_{rr} g_{\phi\phi}}}, \end{aligned} \tag{14}$$

where, $s = S/m$ represents the specific spin angular momentum of the particle, which can be positive or negative depending on the direction of p_ϕ.

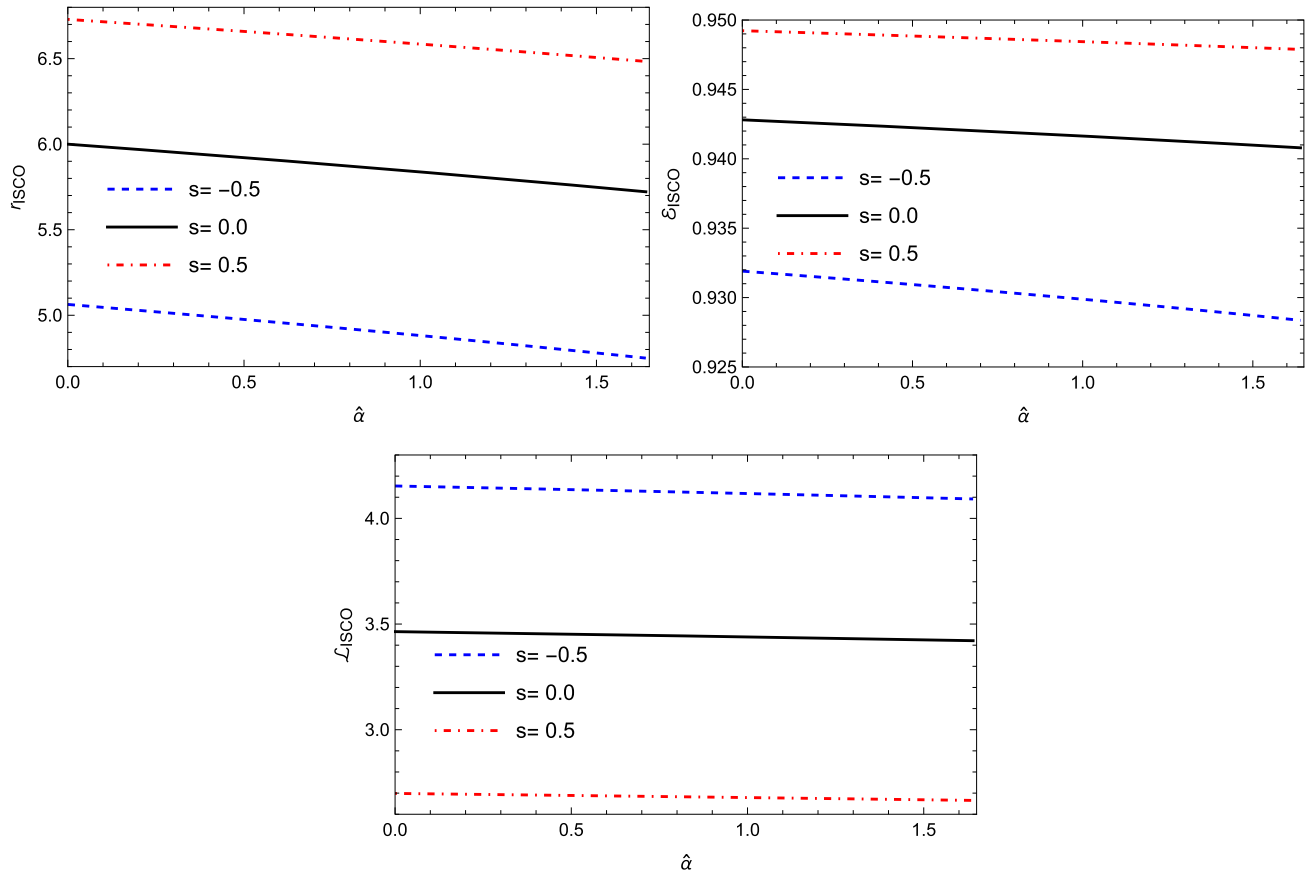

Fig. 5 The variation of the radius, specific angular momentum, and energy at the ISCO with respect to the parameter $\hat{\alpha}$ of the BH for various particle spin values

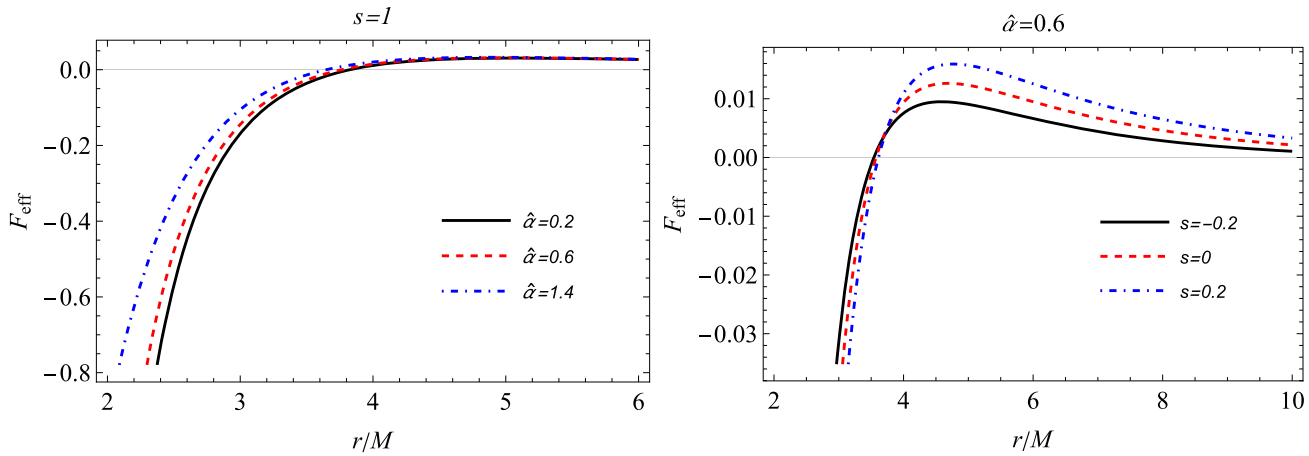

Fig. 6 Effective force as a function of radial distance in various spin parameter s and $\hat{\alpha}$

Substituting Eq. (14) into Eq. (13) and performing basic calculations, the formulations for energy E and total angular momentum J can be reformulated as:

$$\begin{aligned} -E &= p_t - \frac{s p_\phi g_{tt,r}}{2\sqrt{-g_{tt}g_{rr}g_{\phi\phi}}} = p_t + \frac{s}{2r} f'(r) p_\phi \\ J &= p_\phi + \frac{s p_t g_{\phi\phi,r}}{2\sqrt{-g_{tt}g_{rr}g_{\phi\phi}}} = p_\phi + s p_t. \end{aligned} \tag{15}$$

By solving the above system for p_t and p_ϕ, one can easily get the following results:

$$\begin{aligned} p_t &= \frac{\mathcal{J}Ms\left(2\alpha M - r^3\right) - Er^6}{2\alpha M^2 s^2 - Mr^3 s^2 + r^6}, \\ p_\phi &= \frac{r^6(Es + \mathcal{J})}{2\alpha M^2 s^2 - Mr^3 s^2 + r^6}. \end{aligned} \tag{16}$$

Now, from Eq. (6), one can get the expression for the radial canonical momentum as:

$$(p^r)^2 = -g^{rr}[g^{tt}p_t^2 + g^{\phi\phi}p_\phi^2 + m^2]. \tag{17}$$

By substituting Eq. (16) and the components of the metric tensor into Eq. (17), one can easily derive the quadratic equation for the energy E of the spinning particle [64,65] as:

$$\rho(u^r)^2 = \alpha\mathcal{E}^2 + \delta\mathcal{E} + \gamma, \tag{18}$$

where,

$$\alpha = 4[r^2 - s^2 f(r)], \tag{19}$$

$$\delta = 4s\mathcal{J}[-2f(r) + f'(r)r], \tag{20}$$

$$\gamma = \mathcal{J}^2\left[f'(r)^2 s^2 - 4f(r)\right] - f(r)\left[2r - f'(r)s^2\right]^2 \tag{21}$$

$$\rho = \left[2r - f'(r)s^2\right]^2. \tag{22}$$

Now, in further calculations, one can use the following dimensionless variables: $\mathcal{J} = \frac{J}{mM}$, $\int = \frac{\mathcal{S}}{mM}$, $\mathcal{E} = \frac{E}{mM}$. Now, one can rewrite Eq. (18) as:

$$(u^r)^2 = \frac{\alpha}{\rho}(\mathcal{E} - V_+)(\mathcal{E} - V_-). \tag{23}$$

To achieve the circular motion of the spinning particles, we impose the condition $p^r = 0$, from which we can define the effective potential [36,43] in the following manner:

$$V_\pm = \frac{-\delta \pm \sqrt{\delta^2 - 4\alpha\gamma}}{2\alpha}. \tag{24}$$

One can define the effective potential under the following assumption that spinning particles possess positive energy: $V_{eff} = E_+$. Figure 2 demonstrates the radial dependence of the effective potential at fixed $\mathcal{L} = 3.5$ for different values of the parameter $\hat{\alpha}$ and s. The upper row of the plot shows the dependence of the effective potential on the radial motion of the spinning particle for different values of s, with the parameter fixed at $\hat{\alpha} = 0.6$ and $\hat{\alpha} = 0.9$. An increase in the parameter $\hat{\alpha}$ results in an increase in the effective potential. In contrast, the bottom row of the plot depicts the influence of the various values of the parameter $\hat{\alpha}$ on the effective potential at a fixed value $s = 0.2$ and $s = -0.2$. As r/M increases, V_{eff} approaches an asymptotic value, indicating stable behavior at large radial distances. We can see from the graph that, if s increase V_{eff} is also increases significantly. The bottom graphs show that for different values of the parameter $\hat{\alpha}$, V_{eff} is nearly similar at large radial distances.

3.2 Innermost stable circular orbit

We now examine the dynamics of a spinning particle in spacetime (1) by identifying the stable circular orbits, which are consistently the focal point of attention. It is widely recognized that two conditions must be satisfied for circular orbits:

(i) $dr/d\tau = 0$ or $\mathcal{E} = V_{eff}(r)$ (the motion with a constant radius R) and (ii) $d^2r/d\tau^2 = 0$ or $V'_{eff}(r) = 0$ (the motion with zero acceleration). However, these constraints alone do not ensure the stability of circular orbits. To guarantee stability, the second radial derivative of the effective potential must be positive, specifically $d^2V_{eff}/dr^2 \geq 0$. Moreover, the equality of the last condition signifies the ISCO.

So, the dependence of the ISCO radius, the specific angular momentum, and the specific energy at ISCO on the spin s for different values of $\hat{\alpha}$, is presented in Fig. 4. The graphs indicate that for small values of s, an increase in the para decrease in both the radius $r_{\mathcal{ISCO}}$ and the specific energy $E_{\mathcal{ISCO}}$, while the specific angular momentum $L_{\mathcal{ISCO}}$ increases. Beyond a certain value of s, the curves for larger values of $\hat{\alpha}$ cross over and switch positions with those for smaller $\hat{\alpha}$. This suggests a complex interaction between $\hat{\alpha}$ and s, possibly due to dynamic changes in orbital stability and spacetime geometry at high spin. Moreover, the third graph of the specific energy is of particular interest. As observed, the ISCO energy is independent of the parameter $\hat{\alpha}$ to $s \approx 1.5$ and begins to differ noticeably only after $s \approx 1.5$. Additionally, the vertical lines in Fig. 4 define *the superluminal bound*, the maximum values of the spin s, after which the values of the ISCO are non-physical. In other words, the left side of the lines corresponds to the time-like particles, while the right side represents space-like particles, which lacks physical meaning. Furthermore, the influence of the same physical quantities ($r_{\mathcal{ISCO}}$, $\mathcal{L}_{\mathcal{ISCO}}$), and $\mathcal{E}_{\mathcal{ISCO}}$ on the parameter α for different values of spin s is illustrated in Fig. 5. The plot illustrates a linear relationship between $r_{\mathcal{ISCO}}$ and $\mathcal{E}_{\mathcal{ISCO}}$ with respect to $\hat{\alpha}$, and a rise in spin s results in higher function values. The dependence of the particle's angular momentum $\mathcal{L}_{\mathcal{ISCO}}$ on $\hat{\alpha}$ remains largely unaffected. In Fig. 3, the variation of the critical spin values s_{max} with respect to $\hat{\alpha}$ is presented. Clearly, when the $\hat{\alpha}$ parameter increases, the critical value of the spin also increases.

3.3 Effective force

The effective force acting on a particle reveals its motion, indicating whether it is being attracted toward the BH or moving away from it. We examine the spinning particle's motion around quantum-corrected BH, where both attractive and repulsive gravitational forces can occur. Using the expression for V_{eff}, we determine the effective force acting on the particles, which is given by

$$F = -\frac{1}{2}\frac{dV_{eff}}{dr}. \tag{25}$$

The behavior of the effective force around the quantum-corrected BH is shown in Fig. 6, as a function of r, for the parameter of varying values of $\hat{\alpha}$ and spin s. It is noted that the effective force acting on the particles has the same behavior for both the parameters $\hat{\alpha}$ and the parameters s. The effective force is small when the parameter $\hat{\alpha}$ or the spin parameter s has small values, however, the effective force increases when the parameter $\hat{\alpha}$ or s increases. When we fix s and vary $\hat{\alpha}$, the effective force radial profiles coincide as the radial distance r increases. However, for varying values of $\hat{\alpha}$, different radial profiles of the effective force can be observed as the radial distance r increases.

4 Collision of spinning particles

This section is devoted to investigating the head-on collision of two particles near the horizon of the BH and the ultra-high energy produced by it. Here, we assume that particles coming from infinity fall freely and produce a head-on collision near the horizon of the BH. For this, we first analyze the particle's angular momentum, which is extremely important.

4.1 Angular momentum

It is worth mentioning that, to produce a head-on collision of two particles, we need to know the critical values of the angular momentum of the particle for which the collision is possible. In order to find these values of the angular momentum L_{cr}, the following conditions should be satisfied:

(i) $\dot{r}^2 = 0$;
(ii) $d\dot{r}^2/dr = 0$.

Obviously, particles with an angular momentum higher than the critical values cannot approach the BH and produce a collision.

Figure 7 shows the critical angular momentum of a spinning particle as a function of spin s and the parameter $\hat{\alpha}$. The first graph shows that the limiting values of the angular momentum L_{cr} decrease slightly when $\hat{\alpha}$ increases. In addition, for fixed $\hat{\alpha}$, the values of the critical angular momentum decrease with increasing spin s.

The behavior of L_{cr} in terms of $\hat{\alpha}$ for various values of spin s is shown in the second graph of Fig. 7. It is clear from the graph that the dependence of L_{cr} on $\hat{\alpha}$ is linear and gradually decreasing, and a rise in the spin s gives a negative shift in the critical angular momentum.

4.2 The center-of-mass energy of spinning particles

Now, we utilize the following expression for computing the center-of-mass energy E_{cm} of the colliding spinning particles:

$$\begin{aligned} E_{cm}^2 &= -g^{\mu\nu}(p_\mu^{(1)} + p_\mu^{(2)})(p_\nu^{(1)} + p_\nu^{(2)}) \\ &= m_1^2 + m_2^2 - 2g^{\mu\nu}p_\mu^{(1)}p_\nu^{(2)}, \end{aligned} \tag{26}$$

where $p_\mu^{(1)}$ and $p_\mu^{(2)}$ are four-momentum of spinning particles, respectively (see Eqs. (16), and (17)). Here, we assume that particles have the same mass $m_1 = m_2 = m$, but different four-momenta $p_\mu^{(1)}$ and $p_\mu^{(2)}$. Thus, the final expression for the center-of-mass energy of colliding particles has the form:

$$\begin{aligned} \mathcal{E}_{cm}^2 &= \frac{E^2}{2m^2} \\ &= 1 - \frac{g^{tt}p_t^{(1)}p_t^{(2)} + g^{rr}p_r^{(1)}p_r^{(2)} + g^{\varphi\varphi}p_\varphi^{(1)}p_\varphi^{(2)}}{m^2}. \end{aligned} \tag{27}$$

The radial dependence of the center-of-mass energy E_{cm} of the spinning particles for different values of spin s at fixed $\hat{\alpha} = 0.6$ is given in Fig. 8. It consists of six panels divided into three columns, each of which has the same fixed value of the spin of the first particle while varying the values of the second one. The first column illustrates the case of a spinless particle that interacts with both positively and negatively spinning particles. By comparing these graphs, we observe that a spinless particle interacting with a negatively spinning particle yields a higher center-of-mass energy than when interacting with a positively spinning particle. The middle column presents interactions between a negatively spinning particle and both a positively and negatively spinning one. It is evident that the interaction between two negatively spinning particles results in a higher released energy than the interaction between a negatively and positively spinning particle. The third column of the graphs shows the dependence of the center-of-mass energy for the first positively spinning particle $s = 1.0$ with different positively and negatively spinning particles. The results indicate that a positively spinning particle interacting with a negatively spinning particle produces the highest center-of-mass energy among the cases considered.

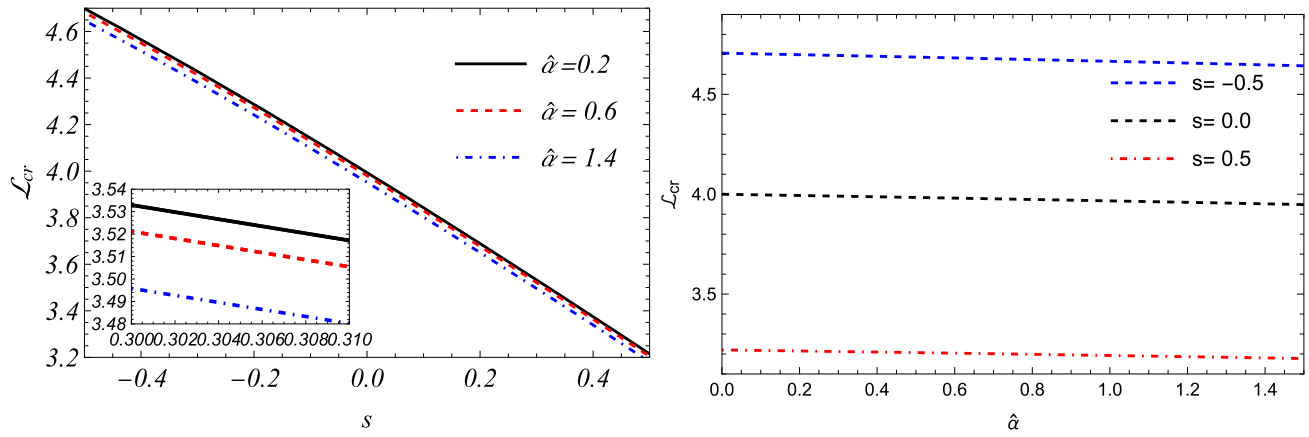

Fig. 7 Dependence of critical angular momentum on the spin s and $\hat{\alpha}$

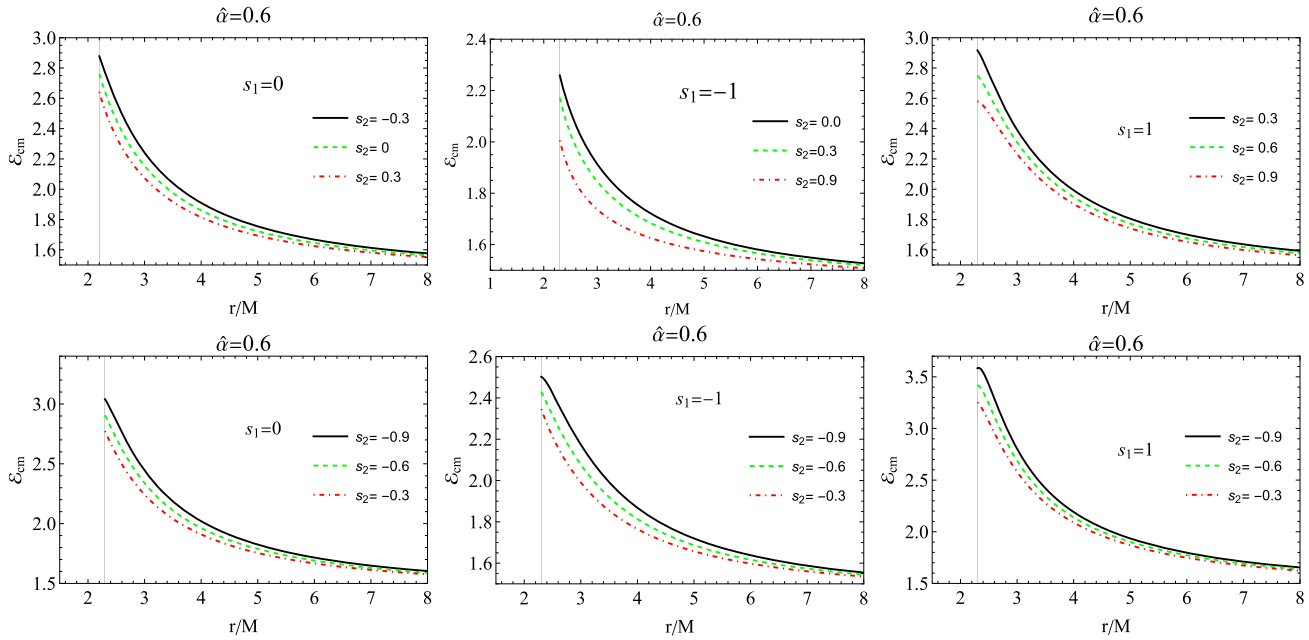

Fig. 8 The radial dependence of the center-of-mass energy of spinning particles for different values of the spin at fixed $\hat{\alpha} = 0.6$

5 Conclusions

This paper is devoted to investigating the spinning particle motion around a quantum -corrected BH. In summary, the following results should be emphasized below:

- Initially, we have examined the fundamental principles of spinning particle motion using the MPD equations.
- The effective potential V_{eff} of the spinning particle has been computed and its radial dependency has been graphed for various parameter values of $\hat{\alpha}$ and s. Consequently, both parameters increase the effective potential.
- Furthermore, the influence of parameters $\hat{\alpha}$ and spin s on the ISCO has been examined. The presence of the parameter $\hat{\alpha}$ reduces the radius of the ISCO. The influence of the same parameters on the angular momentum and energy at ISCO has been observed. The presence and variation of the parameter $\hat{\alpha}$ increase the specific angular momentum while diminishing the energy at the ISCO up to the joining point.
- Moreover, constraints on spin s (the *superluminal bound condition*) have been identified, beyond which the particle's trajectory becomes space-like and non-physical. The relationship between the critical values of spin s_{max} and $\hat{\alpha}$ has been illustrated and analyzed.
- We have also analyzed the effective force surrounding the quantum-corrected BHs as a function of r, for different values of the parameters $\hat{\alpha}$ and s. The effective force

acting on the particles exhibits a similar trend for both the parameter $\hat{\alpha}$ and the spin parameter s. Specifically, the effective force is minimal when $\hat{\alpha}$ or s is small but increases as these parameters grow. When the parameter s is maintained constant and the BH parameter $\hat{\alpha}$ is varied, the radial profiles of the effective force converge as the radial distance r increases. However, for different values of s, distinct radial profiles of the effective force can be observed as the radial distance r increases.

- The collision of two spinning particles in proximity to a quantum-corrected BH has been examined. We have determined the critical values of the angular momentum of the spinning particle, L_{cr}, and found that an increase in $\hat{\alpha}$ and s results in its decrease .
- Finally, we have illustrated the radial dependence of the center-of-mass energy $\mathcal{E}_{cm}$ of spinning particles for various values of s. The center-of-mass energy reaches its highest value when one spinning particle has positive spin and the other has negative spin.

Our work indicates substantial effects of quantum corrections and spinning particle dynamics; however, the comprehensive implications of higher-order quantum gravity corrections are still unexamined. Future research may expand our current analysis to encompass non-equatorial motion and examine the effects of different parameters on spinning particle motion.

Acknowledgements This research is partly supported by Research Grant F-FA-2021-510 of the Uzbekistan Ministry for Innovative Development. The work of PC was financially supported by Walailak University under the project titled "*Invitation of World Renowned Scholars for Promotion of Walailak University's International Research Collaborations 2025*".

Data Availability Statement My manuscript has no associated data. [Author's' comment: There is no observational data related to this article. The necessary calculations and graphical discussions are already available in the manuscript.]

Code Availability Statement My manuscript has no associated code/software. [Author's comment: There is no specific code and software.]

Funded by SCOAP[3].

References

1. K. Akiyama et al., ApJ **875**, L1 (2019). https://doi.org/10.3847/2041-8213/ab0ec7. arXiv:1906.11238 [astro-ph.GA]
2. K. Akiyama et al., Astrophys. J. Lett **930**, L12 (2022). https://doi.org/10.3847/2041-8213/ac6674
3. B.P. Abbott et al., Phys. Rev. D **100**, 104036 (2019). https://doi.org/10.1103/PhysRevD.100.104036. arXiv:1903.04467 [gr-qc]
4. T. Johannsen, D. Psaltis, Phys. Rev. D **83**, 124015 (2011). https://doi.org/10.1103/PhysRevD.83.124015
5. L. Rezzolla, A. Zhidenko, Phys. Rev. D **90**, 084009 (2014). https://doi.org/10.1103/PhysRevD.90.084009
6. R. Konoplya, L. Rezzolla, A. Zhidenko, Phys. Rev. D **93**, 064015 (2016). https://doi.org/10.1103/PhysRevD.93.064015
7. R. Ruffini, J.A. Wheeler, Phys. Today **24**, 30 (1971). https://doi.org/10.1063/1.3022513
8. S.W. Hawking, Commun. Math. Phys. **25**, 152 (1972). https://doi.org/10.1007/BF01877517
9. S.W. Hawking, M.J. Perry, A. Strominger, Phys. Rev. Lett. **116**, 231301 (2016). https://doi.org/10.1103/PhysRevLett.116.231301. arXiv:1601.00921 [hep-th]
10. J. Ovalle, R. Casadio, E. Contreras, A. Sotomayor, Phys. Dark Universe **31**, 100744 (2021). https://doi.org/10.1016/j.dark.2020.100744. arXiv:2006.06735 [gr-qc]
11. A. Ditta, S. Mumtaz, G. Mustafa, S.K. Maurya, F. Atamurotov, A. Mahmood, J. High Energy Astrophys. **42**, 146 (2024). https://doi.org/10.1016/j.jheap.2024.04.007
12. A. Ditta, F. Javed, S.K. Maurya, G. Mustafa, F. Atamurotov, Phys. Dark Universe **42**, 101345 (2023). https://doi.org/10.1016/j.dark.2023.101345
13. T.P. Sotiriou, V. Faraoni, Phys. Rev. Lett. **108**, 081103 (2012). https://doi.org/10.1103/PhysRevLett.108.081103. arXiv:1109.6324 [gr-qc]
14. E. Babichev, C. Charmousis, J. High Energy Phys. **2014**, 106 (2014). https://doi.org/10.1007/JHEP08(2014)106. arXiv:1312.3204 [gr-qc]
15. A. Cisterna, C. Erices, Phys. Rev. D **89**, 084038 (2014). https://doi.org/10.1103/PhysRevD.89.084038. arXiv:1401.4479 [gr-qc]
16. T.P. Sotiriou, S.-Y. Zhou, Phys. Rev. Lett. **112**, 251102 (2014). https://doi.org/10.1103/PhysRevLett.112.251102. arXiv:1312.3622 [gr-qc]
17. G. Antoniou, A. Bakopoulos, P. Kanti, Phys. Rev. Lett. **120**, 131102 (2018). https://doi.org/10.1103/PhysRevLett.120.131102. arXiv:1711.03390 [hep-th]
18. D. Grumiller, A. Pérez, M.M. Sheikh-Jabbari, R. Troncoso, C. Zwikel, Phys. Rev. Lett. **124**, 041601 (2020). https://doi.org/10.1103/PhysRevLett.124.041601. arXiv:1908.09833 [hep-th]
19. C. Martínez, R. Troncoso, J. Zanelli, Phys. Rev. D **70**, 084035 (2004). https://doi.org/10.1103/PhysRevD.70.084035. arXiv:hep-th/0406111 [gr-qc]
20. C. Herdeiro, E. Radu, Int. J. Mod. Phys. D **24**, 1542014–219 (2015). https://doi.org/10.1142/S0218271815420146. arXiv:1504.08209 [gr-qc]
21. M. Bañados, J. Silk, S.M. West, Phys. Rev. Lett. **103**, 111102 (2009). https://doi.org/10.1103/PhysRevLett.103.111102
22. M. De Laurentis, Z. Younsi, O. Porth, Y. Mizuno, L. Rezzolla, Phys. Rev. D **97**, 104024 (2018). https://doi.org/10.1103/PhysRevD.97.104024. arXiv:1712.00265 [gr-qc]
23. S.R. Shaymatov, B.J. Ahmedov, A.A. Abdujabbarov, Phys. Rev. D **88**, 024016 (2013). https://doi.org/10.1103/PhysRevD.88.024016
24. V.P. Frolov, P. Krtouš, Phys. Rev. D **83**, 024016 (2011). https://doi.org/10.1103/PhysRevD.83.024016. arXiv:1010.2266 [hep-th]
25. G.Z. Babar, F. Atamurotov, S. Ul Islam, S.G. Ghosh, Phys. Rev. D **103**, 084057 (2021). https://doi.org/10.1103/PhysRevD.103.084057. arXiv:2104.00714 [gr-qc]

26. A. Abdujabbarov, B. Ahmedov, A. Hakimov, Phys. Rev. D **83**, 044053 (2011). https://doi.org/10.1103/PhysRevD.83.044053. arXiv:1101.4741 [gr-qc]
27. F. de Felice, F. Sorge, S. Zilio, Class. Quantum Gravity **21**, 961 (2004). https://doi.org/10.1088/0264-9381/21/4/016
28. A. Nosirov, F. Atamurotov, G. Rakhimova, A. Abdujabbarov, Eur. Phys. J. Plus **138**, 846 (2023). https://doi.org/10.1140/epjp/s13360-023-04501-4
29. K. Haydarov, J. Rayimbaev, A. Abdujabbarov, S. Palvanov, D. Begmatova, Eur. Phys. J. C **80**, 399 (2020). https://doi.org/10.1140/epjc/s10052-020-7992-9. arXiv:2004.14868 [gr-qc]
30. F. Atamurotov, M. Alloqulov, A. Abdujabbarov, B. Ahmedov, Eur. Phys. J. Plus **137**, 634 (2022). https://doi.org/10.1140/epjp/s13360-022-02846-w
31. F. Atamurotov, D. Ortiqboev, A. Abdujabbarov, G. Mustafa, Eur. Phys. J. C **82**, 659 (2022). https://doi.org/10.1140/epjc/s10052-022-10619-z
32. A.N. Aliev, N. Özdemir, MNRAS **336**, 241 (2002). https://doi.org/10.1046/j.1365-8711.2002.05727.x. arXiv:gr-qc/0208025
33. M. Jamil, S. Hussain, B. Majeed, Eur. Phys. J. C **75**, 24 (2015). https://doi.org/10.1140/epjc/s10052-014-3230-7. arXiv:1404.7123 [gr-qc]
34. B. Narzilloev, J. Rayimbaev, S. Shaymatov, A. Abdujabbarov, B. Ahmedov, C. Bambi, Phys. Rev. D **102**, 044013 (2020). https://doi.org/10.1103/PhysRevD.102.044013. arXiv:2007.12462 [gr-qc]
35. J. Kovář, P. Slaný, C. Cremaschini, Z. Stuchlík, V. Karas, A. Trova, Phys. Rev. D **90**, 044029 (2014). https://doi.org/10.1103/PhysRevD.90.044029. arXiv:1409.0418 [gr-qc]
36. B. Toshmatov, D. Malafarina, Phys. Rev. D **100**, 104052 (2019). https://doi.org/10.1103/PhysRevD.100.104052. arXiv:1910.11565 [gr-qc]
37. O. Zelenka, G. Lukes-Gerakopoulos, V. Witzany, O. Kopáček, Phys. Rev. D **101**, 024037 (2020). https://doi.org/10.1103/PhysRevD.101.024037. arXiv:1911.00414 [gr-qc]
38. C. Conde, C. Galvis, E. Larrañaga, Phys. Rev. D **99**, 104059 (2019). https://doi.org/10.1103/PhysRevD.99.104059. arXiv:1905.01323 [gr-qc]
39. C.A. Benavides-Gallego, W.-B. Han, D. Malafarina, B. Ahmedov, A. Abdujabbarov, Phys. Rev. D **104**, 084024 (2021). https://doi.org/10.1103/PhysRevD.104.084024. arXiv:2107.07998 [gr-qc]
40. F. Abdulxamidov, C.A. Benavides-Gallego, W.-B. Han, J. Rayimbaev, A. Abdujabbarov, Phys. Rev. D **106**, 024012 (2022). https://doi.org/10.1103/PhysRevD.106.024012. arXiv:2205.11727 [gr-qc]
41. J.M. Ladino, E. Larrañaga, Int. J. Mod. Phys. D **31**, 2250091 (2022). https://doi.org/10.1142/S0218271822500912. arXiv:2302.12213 [gr-qc]
42. E. Hackmann, C. Lämmerzahl, Y.N. Obukhov, D. Puetzfeld, I. Schaffer, Phys. Rev. D **90**, 064035 (2014). https://doi.org/10.1103/PhysRevD.90.064035. arXiv:1408.1773 [gr-qc]
43. F. Abdulxamidov, J. Rayimbaev, A. Abdujabbarov, Z. Stuchlík, Phys. Rev. D **108**, 044030 (2023). https://doi.org/10.1103/PhysRevD.108.044030. arXiv:2308.05392 [gr-qc]
44. F. Abdulxamidov, C.A. Benavides-Gallego, B. Narzilloev, I. Hussain, A. Abdujabbarov, B. Ahmedov, H. Xu, Eur. Phys. J. Plus **138**, 635 (2023). https://doi.org/10.1140/epjp/s13360-023-04283-9
45. P.I. Jefremov, O.Y. Tsupko, G.S. Bisnovatyi-Kogan, Phys. Rev. D **91**, 124030 (2015). https://doi.org/10.1103/PhysRevD.91.124030. arXiv:1503.07060 [gr-qc]
46. I. Timogiannis, G. Lukes-Gerakopoulos, T.A. Apostolatos, Phys. Rev. D **104**, 024042 (2021). https://doi.org/10.1103/PhysRevD.104.024042. arXiv:2104.11183 [gr-qc]
47. A. Davlataliev, J. Rayimbaev, F. Abdulkhamidov, Z. Stuchlik, A. Abdujabbarov, Phys. Dark Universe **46**, 101590 (2024). https://doi.org/10.1016/j.dark.2024.101590
48. T. Oteev, F. Abdulkhamidov, J. Rayimbaev, Z. Stuchlík, B. Ahmedov, Phys. Dark Universe **46**, 101588 (2024). https://doi.org/10.1016/j.dark.2024.101588
49. V. Skoupý, G. Lukes-Gerakopoulos, L.V. Drummond, S.A. Hughes, Phys. Rev. D **108**, 044041 (2023). https://doi.org/10.1103/PhysRevD.108.044041. arXiv:2303.16798 [gr-qc]
50. S. Giri, P. Sheoran, H. Nandan, S. Shaymatov, Eur. Phys. J. Plus **138**, 245 (2023). https://doi.org/10.1140/epjp/s13360-023-03848-y. arXiv:2207.06007 [gr-qc]
51. R.M. Plyatsko, O.B. Stefanyshyn, M.T. Fenyk, Class. Quantum Gravity **28**, 195025 (2011). https://doi.org/10.1088/0264-9381/28/19/195025. arXiv:1110.1967 [gr-qc]
52. M. Mathisson, Acta Phys. Polon. **6**, 163 (1937)
53. A. Papapetrou, Proc. R. Soc. Lond. A **209**, 248 (1951). https://doi.org/10.1098/rspa.1951.0200
54. E. Corinaldesi, A. Papapetrou, Proc. R. Soc. Lond. A **209**, 259 (1951). https://doi.org/10.1098/rspa.1951.0201
55. M. Bañados, J. Silk, S.M. West, Phys. Rev. Lett. **103**, 111102 (2009). https://doi.org/10.1103/PhysRevLett.103.111102. arXiv:0909.0169 [hep-ph]
56. W. Guzmán-Ramírez, R. Becerril, S. Valdez-Alvarado, A.A. Deriglazov, Phys. Rev. D **105**, 124036 (2022). https://doi.org/10.1103/PhysRevD.105.124036. arXiv:2111.07996 [gr-qc]
57. M.U. Shahzad, S. Khalid, A. Övgün, Eur. Phys. J. C **83**, 1031 (2023). https://doi.org/10.1140/epjc/s10052-023-12211-5
58. J.M. Ladino, C. Andrés del Valle, E. Larrañaga, (2023). arXiv e-prints https://doi.org/10.48550/arXiv.2302.12352. arXiv:2302.12352 [gr-qc]
59. J.M. Ladino, C.A. Benavides-Gallego, E. Larrañaga, J. Rayimbaev, F. Abdulxamidov, Eur. Phys. J. C **83**, 989 (2023). https://doi.org/10.1140/epjc/s10052-023-12187-2. arXiv:2305.15350 [gr-qc]
60. J. Lewandowski, Y. Ma, J. Yang, C. Zhang, Phys. Rev. Lett. **130**, 101501 (2023). https://doi.org/10.1103/PhysRevLett.130.101501. arXiv:2210.02253 [gr-qc]
61. S. Yang, Y.-P. Zhang, T. Zhu, L. Zhao, Y.-X. Liu, J. Cosmol. Astropart. Phys. **2025**, 091 (2025). https://doi.org/10.1088/1475-7516/2025/01/091. arXiv:2407.00283 [gr-qc]
62. C. Rovelli, *Quantum Gravity, Cambridge Monographs on Mathematical Physics* (Cambridge University Press, Cambridge, 2004)
63. W. Tulczyjew, Acta Phys. Polon. **18**, 393 (1959)
64. F. Abdulxamidov, J. Rayimbaev, A. Abdujabbarov, Z. Stuchlík, Phys. Rev. D **108**, 044030 (2023). https://doi.org/10.1103/PhysRevD.108.044030
65. B. Toshmatov, D. Malafarina, Phys. Rev. D **100**, 104052 (2019). https://doi.org/10.1103/PhysRevD.100.104052